NANO LETTERS

pubs.acs.org/NanoLett

Nanoscale Thermometry Using Point Contact Thermocouples

Seid Sadat,[†] Aaron Tan,[‡] Yi Jie Chua,[†] and Pramod Reddy[†,*]

[†]Department of Mechanical Engineering and [‡]Department of Materials Science and Engineering, University of Michigan, Ann Arbor, 48109

ABSTRACT Probing temperature fields with nanometer resolution is critical to understanding nanoscale thermal transport as well as dissipation in nanoscale devices. Here, we demonstrate an atomic force microscope (AFM)-based technique capable of mapping temperature fields in metallic films with ~10 mK temperature resolution and <100 nm spatial resolution. A platinum-coated AFM cantilever placed in soft mechanical contact with a metallic (gold) surface is used to sequentially create point contact thermocouples on a grid. The local temperature at each point contact is obtained by measuring the thermoelectric voltage of the platinum−gold point contact and relating it to the local temperature. These results demonstrate a direct measurement of the temperature field of a metallic surface without using specially fabricated scanning temperature-probes.

KEYWORDS Nanoscale thermometry, point contact thermocouple, atomic force microscope, temperature field

Nanoscale thermometry is essential to understand dissipation in a variety of electronic and photonic devices.[1,2] Further, it can also be used in fundamental studies of transport in nanoscale systems.[3,4] Given the broad applicability of nanoscale thermometry, experimental techniques have been developed recently to obtain information regarding temperature fields with nanometer to micrometer resolution.[1,5−8] Among these, techniques based on using an atomic force microscope (AFM) have succeeded in achieving high spatial resolution (~50 nm) along with excellent temperature resolution (~1 mK). However, most of these AFM-based techniques require either the fabrication of special AFM probes with integrated temperature sensors[9,10] or operation in a vacuum environment.[11] Here, we report an AFM-based technique that does not require AFM probes with integrated temperature sensors and allows, under ambient conditions, a direct measurement of the temperature field on a metal surface with excellent thermal and spatial resolutions.

The general strategy adapted in this work for achieving nanoscale temperature resolution is conceptually simple. First, a silicon (Si) AFM cantilever with a tip radius of ~20 nm is deposited with ~5 nm titanium adhesion layer and ~40 nm of platinum (Pt) on both sides of the cantilever. The Pt-coated AFM cantilever is anchored to a thermal reservoir at room temperature (Figure 1) and is placed in soft mechanical contact (~10 nN contact force) with a gold (Au) surface whose temperature field is to be determined. These point contact junctions are estimated to have a contact diameter of ~10 nm and have a well-defined and reproducible electrical conductance. Moreover, for a given pair of metals (Pt−Au in this case) the thermoelectric voltage across the point contact junction is only dependent on the local temperature of the point contact. Therefore, by measuring the thermoelectric voltage across a point contact it is possible to obtain the local temperature. Further, by sequentially making point contacts on a uniformly spaced grid of points on a surface and relating the measured thermoelectric voltage across the point contact to the local temperature at each point, it is possible to map the temperature field of the metallic surface with ~0.01 K temperature resolution and <100 nm spatial resolution. Point contact techniques have been used recently to study thermoelectric properties of semiconductors with nanometer resolution.[12] However, until now they have not been used to map temperature fields of surfaces with nanoscale resolution. This letter demonstrates the feasibility of the technique described above by directly measuring the temperature field of a gold surface

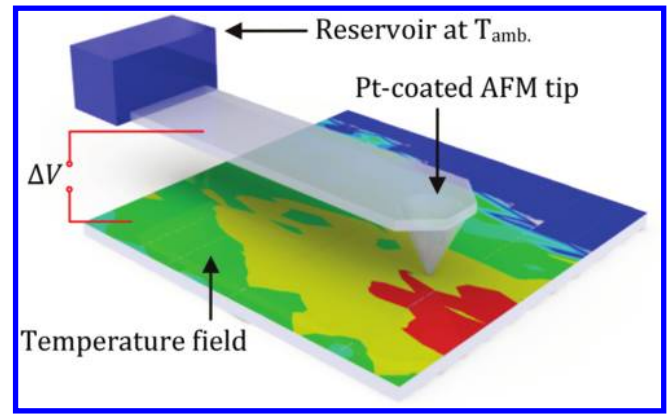

FIGURE 1. Schematic view of the nanoscale point contact thermocouple setup. A Pt-coated AFM cantilever connected to a thermal reservoir at ambient temperature on one end is brought into soft mechanical contact with a metallic surface whose temperature field is to be determined.

* To whom correspondence should be addressed. E-mail: pramodr@umich.edu.
Received for review: 4/16/2010
Published on Web: 06/15/2010

DOI: 10.1021/nl101354e | *Nano Lett.* **2010,** *10,* 2613–2617

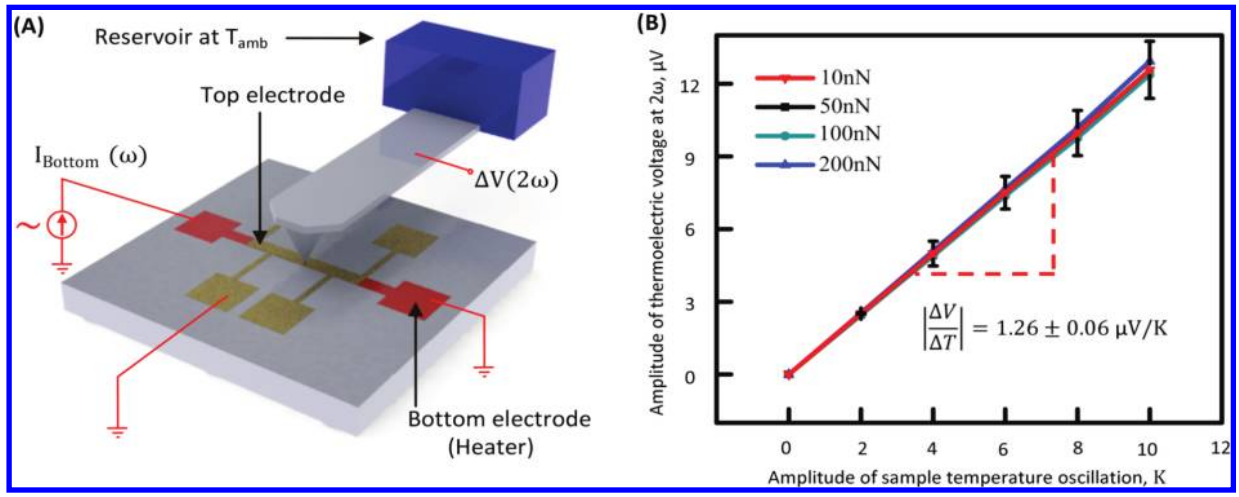

FIGURE 2. (A) Schematic view of point contact thermocouple characterization setup (not drawn to scale/proportion). A sinusoidal electric current at frequency ω is passed through the bottom electrode, which causes temperature oscillations at 2ω in the top electrode that is electrically isolated from the bottom electrode by a 10 nm thick Al_2O_3 layer. A thermoelectric voltage at 2ω develops across the Pt-coated AFM tip and the top electrode (30 nm thick Au), which is measured using a lock-in amplifier. The top and bottom electrodes' dimensions are length = 1 mm, width = 15 μm, thickness of bottom and top electrodes are 100 and 30 nm, respectively. (B) The amplitude of the measured thermoelectric voltage oscillations at 2ω for a Pt−Au point contact for various known amplitudes of temperature oscillations is shown. Five independent measurements are performed at each force. The error bars represent the standard deviations from the mean value for the experiments performed with a contact force of 10 nN.

in which thermal gradients are established. A detailed description of the experimental technique is presented next.

To relate the local temperature of a gold surface to the measured thermoelectric voltage across Pt−Au point contacts, it is essential to first calibrate the point contact thermocouple. This calibration is accomplished by using a microfabricated heater shown in Figure 2A. The microfabricated heater consists of a 1 mm long, 100 nm thick and 10 μm wide gold line that is connected to large contact pads and is patterned on a 500 nm thick thermally grown silicon dioxide (SiO_2) film on a silicon substrate. This gold line (called the bottom gold line in this letter) is later covered with a 10 nm thick layer of aluminum oxide (Al_2O_3), which completely covers the bottom gold line. Subsequently, a second layer of Au (30 nm thick) is deposited on the Al_2O_3 and patterned into a long line with approximately the same width and length as the bottom gold line and is aligned to overlap with it. The thin Al_2O_3 layer electrically isolates the top and bottom lines enabling the measurements described here.

The calibration process consists of two steps. In the first step, a sinusoidal electrical current $I(\omega)$ at a known frequency ω (35 Hz) and an amplitude I_o is passed through the bottom gold electrode, resulting in a temperature oscillation at twice the excitation frequency ($2\omega = 70$ Hz) due to Joule heating.[13] The temperature oscillation in the bottom heater line results in a proportional oscillation in the temperature of the top electrode, which is electrically isolated from the bottom gold line and is grounded through a contact pad on one end (Figure 2A). The amplitude of the temperature oscillations ($\Delta T_{2\omega}$) in the top electrode is experimentally determined by supplying a constant current through the top electrode and monitoring the voltage oscillations ($V_{2\omega}$) across the top electrode at 2ω (Supporting Information) using a lock-in amplifier (SRS-SR830). The temperature oscillations of the top electrode ($\Delta T_{2\omega}$) are then directly related to the voltage oscillation ($V_{2\omega}$) by

$$V_{2\omega} = I_{top} R \alpha \Delta T_{2\omega} \quad (1)$$

where I_{top} is a constant probe current flowing through the top electrode, R and α are the resistance of the top gold line and its temperature coefficient of resistance, respectively; both are experimentally characterized for the samples used in this experiment (Supporting Information). This step in calibration allows us to relate the amplitude of the current in the bottom electrode to the surface temperature of the top electrode.

In the second step of the calibration, the measured thermoelectric voltage across a Pt−Au junction is related to the local temperature of the junction. This is accomplished by placing a Pt-coated AFM cantilever tip in soft mechanical contact (~10 nN) with the top gold line (Figure 2A) whose surface temperature oscillates with a known amplitude as characterized in step 1. Such a point contact has an electrical resistance of ~430 Ω that includes the resistance of the top gold line and the resistance of the Pt film coating the AFM cantilever. The amplitude of the thermoelectric voltage oscillations across the point contact at 2ω (70 Hz) are measured using a lock-in amplifier with a bandwidth of ~1 Hz. The amplitudes of the measured thermoelectric voltages for various amplitudes of surface temperature oscillations are shown in Figure 2B. To study the variation in the thermoelectric voltages for different contacts, measurements were performed on five independent point contacts

DOI: 10.1021/nl101354e | *Nano Lett.* **2010,** *10,* 2613–2617

with a contact force of 10 nN. Figure 2B presents the mean value and standard deviation of the measured thermoelectric voltages for different temperature amplitudes in these five independent experiments. As can be seen from the figure, the measured thermoelectric voltage for any given magnitude of temperature oscillation shows very little variation across the five independent experiments, thus demonstrating the repeatability of the technique. Further, to study the force dependence on the thermoelectric voltage, the calibration measurements were repeated for other applied forces (50, 100, and 200 nN) and the mean values are shown in Figure 2B. These measurements show that the measured thermoelectric voltage is largely independent of the contact force suggesting that the thermoelectric characteristics of Pt−Au point contacts are robust and relatively insensitive to contact forces and the resulting contact geometry. It must be noted that the voltage oscillations (at 2ω) across the point contact are not due to capacitive coupling between the top electrode and the bottom electrode that is excited by an electric current at a frequency ω. In fact control experiments performed by us unambiguously prove this (Supporting Information).

The sensitivity of the point contact thermocouple can be obtained from the slope in Figure 2B ($|\Delta V/\Delta T| = 1.26 \pm 0.06$ μV/K), which represents the amplitude of the thermoelectric voltage oscillation per Kelvin temperature oscillation of the surface. This value is different from the expected thermopower for a bulk Pt−Au junction which is ~6.5 μV/K.[14,15] This discrepancy can be understood by noting that the thickness of the Pt and Au films in these experiments is comparable to the mean free path of electrons in these films, which is known to result in a pronounced suppression in the magnitude of their Seebeck coefficients.[15,16] In addition, based on studies of thermopower in point contacts made from identical metals[17] it is reasonable to expect that the thermopower of Pt−Au point contacts is small (<1 μV/K) in magnitude (Supporting Information). This point contact thermopower is of importance because the temperature differentials exist not only across thin films of Pt and Au but also exist across the nanometer-sized point contact;[18,19] in fact, a detailed computational analysis suggests that a large temperature differential exists across the Pt−Au point contact (Supporting Information). Given the small Seebeck coefficients for thin films and the Pt−Au point contact, the value of the measured $|\Delta V/\Delta T|$ is not unreasonable.

To demonstrate the capability of this technique, a test device (Figure 3A) created to have large temperature gradients on its surface is studied. This device is fabricated as follows: a 100 nm thick gold film is first deposited on a 500 nm thick SiO_2 film that is thermally grown on silicon. The gold film is patterned such that its width varies periodically as shown in Figure 3A. Subsequently, a 10 nm thick layer of Al_2O_3 is deposited on the gold line and finally a second layer of gold, which is 30 nm thick, is deposited on the Al_2O_3 and patterned such that the top gold layer approximately

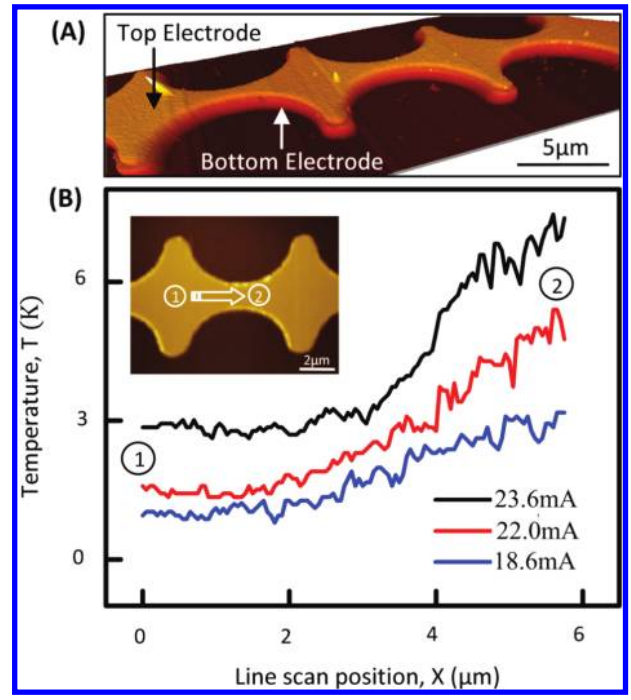

FIGURE 3. (A) Topographical image of the test device with a varying area of cross section. The device features a bottom electrode (100 nm thick) that is electrically isolated from the top electrode (30 nm thick) by a 10 nm thick Al_2O_3 layer. An electric current injected into the bottom electrode leads to temperature gradients in both the bottom electrode and the top electrode. (B) The temperature distribution along a line from point 1 to 2 (shown in inset) is measured with 50 nm spatial resolution for three different bottom electrode heating currents.

overlaps with the bottom gold layer. When an electric current $I(\omega)$ is passed through the bottom gold line that is 100 nm thick, the temperature of the bottom gold line oscillates at 2ω due to Joule heating. Further, thermal gradients are set up in the bottom gold line due to the periodic variation in its cross sectional area, which in turn results in periodic variations in the current density as well as in the volumetric Joule heating. Due to these variations in the current density, the temperature of the narrower regions of the gold line is expected to be higher than those of the wider regions.

The exact distribution of the amplitude of temperature oscillations along a section of the patterned line is experimentally obtained for three different electric currents using the AFM thermal imaging technique described here. This is accomplished by making sequential point contacts separated by 50 nm along a line as shown in Figure 3B. As can be seen from the figure, at any given point the temperature increases with increasing currents. Further, the temperature along the line reaches its maximum value at the narrowest point of the line and is a minimum at its widest point. To demonstrate the ability to determine the spatial temperature distribution on a surface, a section of the device is chosen as shown in Figure 4A (inset) and the temperature of the surface is obtained on a square grid of points with a grid size of 100 nm. The resulting temperature distribution in these

DOI: 10.1021/nl101354e | *Nano Lett.* **2010,** *10,* 2613–2617

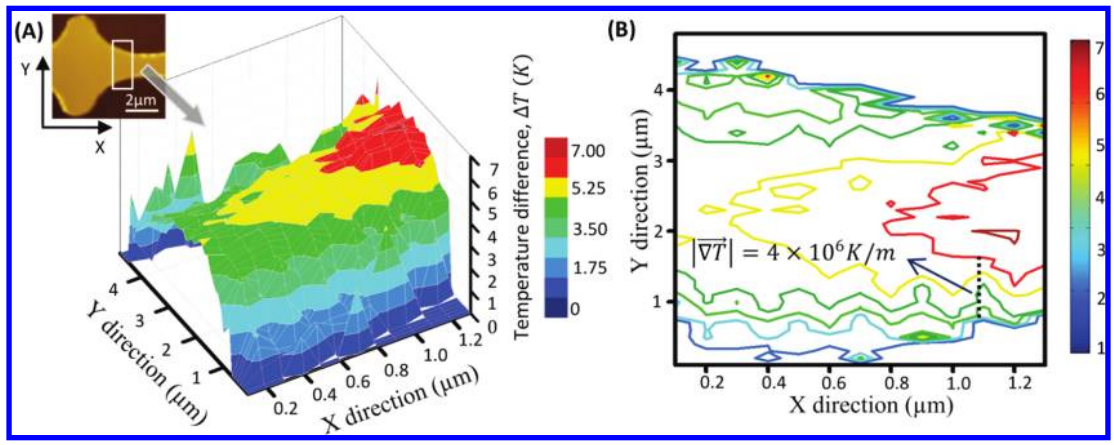

FIGURE 4. (A) Three-dimensional representation of the temperature field in a section of the test device (inset). Temperature is measured on a square grid of points separated by 100 nm without disengaging the tip−substrate contact between consecutive measurements. (B) Isotherm contour plot of the same section of the device. Temperature gradients as large as 4 × 10⁶ K/m are detected in certain regions (shown by a dotted line).

measurements is shown in Figure 4A. The obtained temperature distribution clearly shows that there is a temperature gradient along the section and the temperature increases as the cross sectional area decreases. This unambiguously demonstrates the capability of this point contact thermocouple technique in obtaining spatial resolutions of ∼100 nm.

In this context, an important question that needs to be addressed is the following: what is the ultimate temperature resolution and spatial resolution of this technique? The temperature resolution can be estimated by considering the sensitivity $|\Delta V/\Delta T|$ shown in Figure 2B, and the smallest voltage signal change (ΔV_{min}) that can be reliably detected using the lock-in technique (∼0.01 μV), which is approximately five times larger than the expected Johnson noise. This implies that the smallest temperature change (ΔT_{min}) that can be detected is ∼10 mK ($\Delta T_{min} = \Delta V_{min}/|\Delta V/\Delta T|$). The spatial resolution can be estimated from Figure 4B, which shows a contour plot of the temperature distribution on the section of the device shown in Figure 4A (inset). This plot shows that a temperature gradient $|\vec{\nabla} T|$ of ∼4 × 10⁶ K/m is easily detectable by the method described here. This gradient detection capability in conjunction with the temperature resolution (∼10 mK) would suggest that the spatial resolution of this technique to be ∼2.5 nm ($\Delta r = \Delta T_{min}/|\vec{\nabla} T|$). This temperature resolution is better than or comparable to some of the highest resolutions reported until now[11] for AFM-based measurements where the spatial resolution was estimated using a similar analysis.

However, this estimate needs to be interpreted with caution because of two reasons: (1) the contact diameter of the point contact might be larger than the estimated resolution of ∼2.5 nm, thus reducing the resolution due to spatial averaging, and (2) the inelastic electron mean free path which sets the length scale for thermal equilibration might also be much larger than the estimated resolution of ∼2.5 nm. Given the contact force of ∼10 nN, the contact diameter can be estimated using classical Hertzian theory[1,20]

$$a_{\text{Hertz}} = \left(\frac{6rP}{E^*}\right)^{1/3} \tag{2}$$

where a_{Hertz} is the diameter of contact, r is the tip radius (∼50 nm for Pt-coated tips; see Supporting Information for details), P is the applied load, and $E^* = [(1 - \upsilon_1^2)/E_1 + (1 - \upsilon_2^2)/E_2]^{-1}$, the effective elastic modulus obtained from Young's moduli E_1, E_2, and Poisson's ratios υ_1 and υ_2 of the tip and substrate surface materials. From eq 2, the contact diameter for a platinum-coated tip in contact with a gold surface is estimated to be ∼3 nm. However, if plastic deformation occurs, the contact diameter can be larger and is ∼10 nm (Supporting Information). This diameter is comparable to the length of the inelastic mean free path of the electrons contributing to energy transport in metals (∼20−30 nm for Au),[21] which sets the length scale for thermal equilibration.[22] This discussion suggests that the ultimate resolution of this technique is comparable to the mean free path of electrons in the metallic surface whose temperature field is being probed.

Another important point that must be noted is that due to the small diameter of the point contact the thermal conductance associated with the point contact is also very small (∼1 μW/K, Supporting Information), thus ensuring that the temperature field of the substrate is minimally perturbed. Further, it must be noted that the effect of the small perturbation is already included in the calibration shown in Figure 2 due to which the measured thermoelectric voltage and the inferred temperature is truly representative of the unperturbed temperature field.

While this letter demonstrates the use of this technique to map the temperature fields on a gold surface, this can be potentially adapted to study the temperature fields in other

DOI: 10.1021/nl101354e | *Nano Lett.* **2010,** *10,* 2613–2617

metal surfaces with no native oxide. Further, it should be noted that this technique can also be adapted to study surface temperature fields of dielectrics by depositing ~30 nm thin gold film on the dielectric—provided the temperature distribution in the dielectric is not significantly affected by the thin gold film.

To summarize, this letter demonstrates an AFM-based technique capable of mapping not only the topography but also temperature fields of metallic surfaces with ~10 mK temperature resolution and <100 nm spatial resolution. We believe that this simple but powerful technique, which does not require the fabrication of AFM cantilevers with integrated thermal probes or a vacuum environment, will enable a variety of studies. In fact, we are currently using this powerful technique to study thermal gradients in nanoscale metallic gaps that are of great interest in single molecule studies, and interconnects in nanoscale integrated circuits.

Acknowledgment. We thank Edgar Meyhofer (University of Michigan, Ann Arbor) for helpful discussions. A.T was supported by DOE-BES as part of an EFRC at the University of Michigan (DE-SC0000957). P.R gratefully acknowledges support from the National Science Foundation through a NSF-CAREER award (Award No. 0844902). S.S. would like to thank Leslie George and Edward Tang of the Lurie Nanofabrication Facility (LNF) for their help in fabricating the micro-devices. The LNF is a member of the National Nanotechnology Infrastructure Network and is supported in part by the National Science Foundation.

Supporting Information Available. Experimental details regarding the characterization of the temperature coefficient of resistance of Au thin films, control experiments performed to eliminate the possibility of capacitive coupling, the recipe used for metal (Pt) deposition on AFM cantilevers and a description of the resulting tip radius is provided in the Supporting Information. Further, additional details are provided regarding the temperature profile in the Pt-coated silicon cantilever placed in contact with a hot substrate. A discussion on the relative contributions of the Seebeck coefficients of metal thin films (Au, Pt), and the Pt—Au point contact to the sensitivity $|\Delta V/\Delta T|$ is also provided. This material is available free of charge via the Internet at http://pubs.acs.org.

REFERENCES AND NOTES

(1) Majumdar, A. *Annu. Rev. Mater. Sci.* **1999**, *29*, 505.
(2) Luo, K.; Herrick, R. W.; Majumdar, A.; Petroff, P. *Appl. Phys. Lett.* **1997**, *71*, 1604.
(3) Shi, L.; et al. *Appl. Phys. Lett.* **2000**, *77*, 4295.
(4) Kim, P.; Shi, L.; Majumdar, A.; McEuen, P. L. *Phys. B* **2002**, *323*, 67.
(5) Weaver, J. M. R.; Walpita, L. M.; Wickramasinghe, H. K. *Nature* **1989**, *342*, 783.
(6) Christofferson, J.; Shakouri, A. *Rev. Sci. Instrum.* **2005**, 76.
(7) Fletcher, D. A.; Kino, G. S.; Goodson, K. E. *Microscale Thermophys. Eng.* **2003**, *7*, 267.
(8) Williams, C. C.; Wickramasinghe, H. K. *Appl. Phys. Lett.* **1986**, *49*, 1587.
(9) Luo, K.; Shi, Z.; Lai, J.; Majumdar, A. *Appl. Phys. Lett.* **1996**, *68*, 325.
(10) Mills, G.; et al. *Appl. Phys. Lett.* **1998**, *72*, 2900.
(11) Nakabeppu, O.; et al. *Appl. Phys. Lett.* **1995**, *66*, 694.
(12) Lyeo, H. K.; et al. *Science* **2004**, *303*, 816.
(13) Cahill, D. G. *Rev. Sci. Instrum.* **1990**, *61*, 802.
(14) Dally, J. W.; Riley, W. F.; McConnell, K. G. *Instrumentation for engineering measurements*; Wiley: New York, 1984; p xv.
(15) Salvadori, M. C.; et al. *Appl. Phys. Lett.* **2006**, 88.
(16) Cattani, M.; et al. *J. Appl. Phys.* **2006**, 100.
(17) Weber, L.; Lehr, M.; Gmelin, E. *Phys. B* **1996**, *217*, 181.
(18) Shi, L.; Majumdar, A. *J. Heat. Transfer* **2002**, *124*, 329.
(19) Tan, A.; Sadat, S.; Reddy, P. *Appl. Phys. Lett.* **2010**, 96.
(20) Bietsch, A.; Schneider, M. A.; Welland, M. E.; Michel, B. *J. Vac. Sci. Technol., B* **2000**, *18*, 1160.
(21) Weilmeier, M. K.; Rippard, W. H.; Buhrman, R. A. *Phys. Rev. B* **1999**, *59*, R2521.
(22) Cahill, D. G.; et al. *J. Appl. Phys.* **2003**, *93*, 793.

DOI: 10.1021/nl101354e | *Nano Lett.* **2010,** *10,* 2613--2617